Responses to Referee #3's comments

General comment: This manuscript presents results from a series of chamber experiments investigating the effect of SO_2 on the SOA yield for guaiacol oxidization in the presence of NO_x and seed aerosols. The authors report increased SOA yields for increasing amounts of SO_2 in the chamber and also observe an increased carbon oxidation state. This research is important for understanding the impact of gas-phase precursors on SOA formation, with relevance for severely polluted regions in China. This is a valuable set of experiments, however, the interpretation is not fully supported by the presented results. Before publication, I recommend the authors provide more detailed information on the results from the chamber experiments, as outlined below. These additional data sets will help support the conclusions made in the current manuscript.

Response to comment: Thank you for your constructive comments and valuable suggestions, which would be much helpful to improve the scientific merits of this manuscript. Your concerns have been carefully addressed in the revised manuscript.

Comment 1: The big question I have for this paper is what part of the observations is due to chemical differences (i.e. different SOA formation mechanisms) and what part is due to changes in the physical system (i.e. more seed surface area = more SOA). To understand these results, it would really help to be able to compare the data sets for the experiments. Can you show experimental traces (AMS and PTR-MS) for some of these experiments?

For the particle phase: When/how does the particulate sulfate from SO_2 grow in? What is the NH_4^+ doing? Does it rise as well or is the pH of the particles dropping (forming H_2SO_4) or are you forming organic sulfate? What about the NO^+ and NO_2^+ ions? Do they grow in at the same rate for all experiments? When the lights are turned on for the different experiments, are there any differences in the induction period before SOA growth is observed? How do the chemical properties change with time (What is the time series for the O/C, H/C, and N/C)?

For the gas phase: What do the experimental traces from the PTR-MS look like? Does the decay in Guaiacol look the same in all experiments? Are any other VOC products observed during the experiments? If so, are there any differences between experiments and what do the time series for these products look like? What do the time traces for NO_x and SO_2 look like?

Response to comment 1: In this work, we compared the effect of sulfate formed via SO_2 oxidation on SOA formation with/without seed particles. The results suggested that the physical and chemical factors could be both helpful to enhance SOA yield, but their contributions were very difficult to quantify.

It is well known that sulfate formed via SO_2 oxidation could serve as seed particles (Jaoui et al., 2008) and increase the surface areas of particles (Xu et al., 2016). These roles are favorable to partition more SOA-forming vapors onto particle phase (Zhang et al., 2014), consequently enhancing SOA yields. Therefore, the average gas-particle partitioning timescale ($\overline{\tau}_{\text{g-p}}$) over the course of experiment and the vapor wall-loss timescale ($\tau_{\text{g-w}}$) under different experimental conditions were estimated and discussed in the revised manuscript. Based on $\overline{\tau}_{\text{g-p}} / \tau_{\text{g-w}}$ ratio, the underestimation of SOA yield caused by vapor wall loss could be determined. The calculation methods of $\overline{\tau}_{\text{g-p}}$ and $\tau_{\text{g-w}}$ were added in the Supplement.

For the particle phase: The time-series changes in the concentrations of sulfate and nitrate, as well as ammonium salts are shown in Figure R1 and Figure R2, respectively, which show that the concentrations of sulfate, nitrate, and ammonium salts increase along with the irradiation time. The time-series variations in the concentrations of NO^+ and NO_2^+ ions at different SO_2 concentrations are shown in Figure R3a, and their ratio (NO^+ / NO_2^+) is shown in Figure R3b. Figure 3 shows that the concentrations of NO^+ and NO_2^+ ions are both increase with increasing SO_2 concentration, but the impact of SO_2 on NO^+ / NO_2^+ ratio could be negligible. The induction periods under different conditions are discussed in the revised manuscript (lines 249, 361, and 437-438). For example, the induction period became shorter with the increase of SO_2 concentration (line 249).

The time-series changes in the ratios of O/C, H/C, and N/C are shown in Figures R4-R6. In addition, the time-series variations in the fraction of organic ion groups (CH^+, CHO^+, and CHO_{gt1}^+) are shown in Figure R7, which shows the higher fraction of CHO_{gt1}^+ and lower fraction of CH^+ obtained at higher SO_2 concentration, consequently resulting in higher OS_C of SOA.

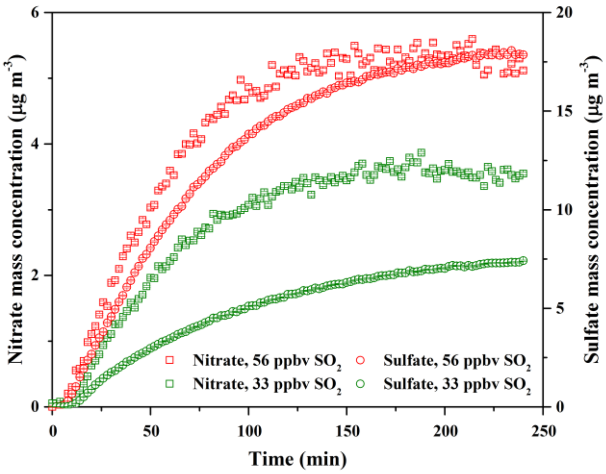

Figure R1. Variations in the concentrations of sulfate and nitrate in the presence of various SO_2 concentrations as a function of reaction time (without seed particles).

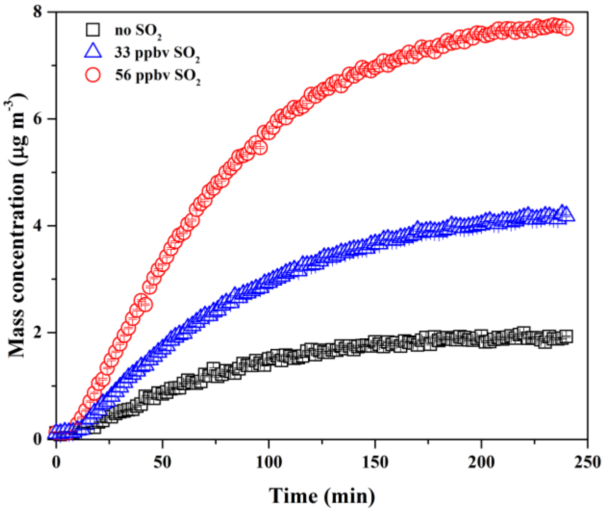

Figure R2. Variations in the concentrations of ammonium salt as function of irradiation time at various SO_2 concentrations (without seed particles).

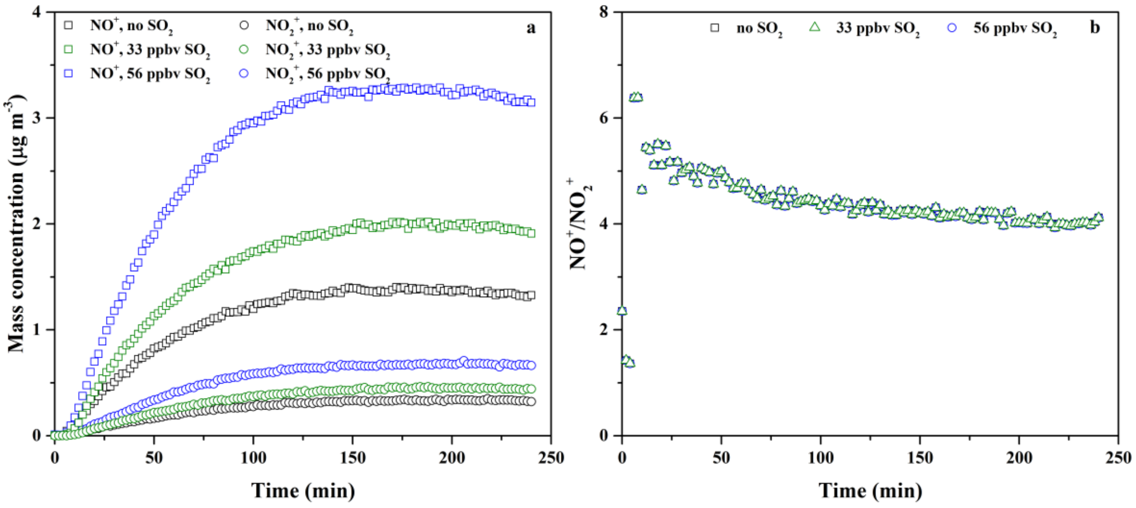

Figure R3. Variations in the mass concentrations of NO^+ and NO_2^+, as well as NO^+/NO_2^+ ratio as a function of irradiation time at various SO_2 concentrations (without seed particles).

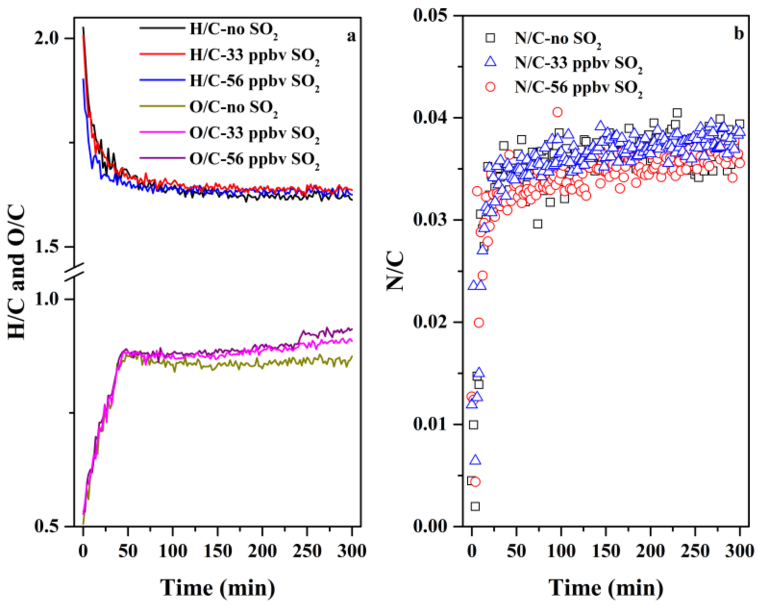

Figure R4. Variations in H/C, O/C, and N/C at various SO_2 concentrations as a function of irradiation time (without seed particles).

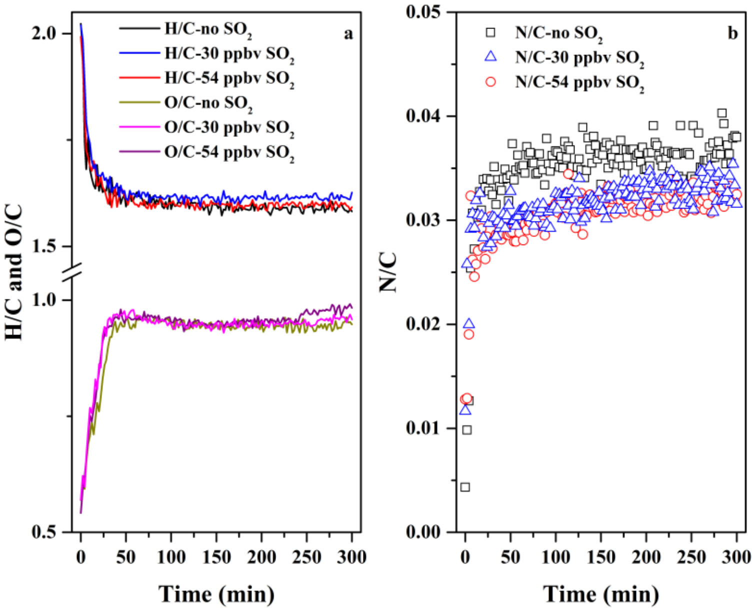

Figure R5. Variations in H/C, O/C, and N/C at various SO_2 concentrations as a function of irradiation time with NaCl seed particles.

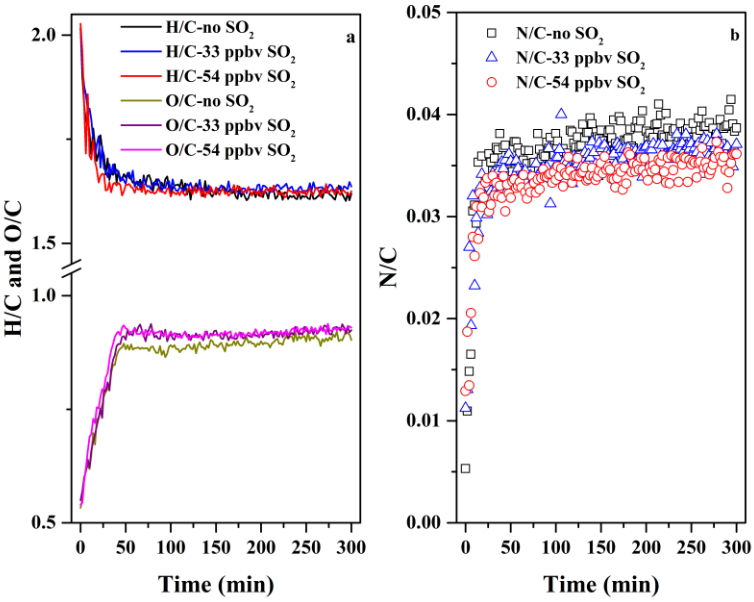

Figure S6. Variations in H/C, O/C, and N/C at various SO_2 concentrations as a function of irradiation time with $(NH_4)_2SO_4$ seed particles.

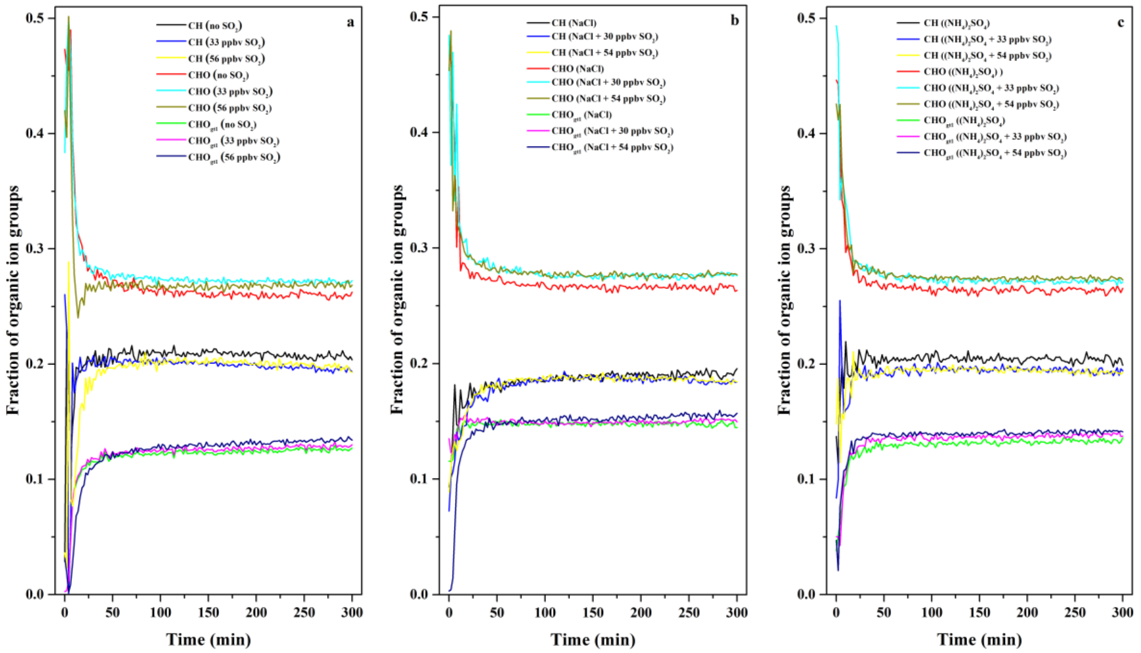

Figure R7. Variations in the fraction of organic ion groups as a function of irradiation time in the presence of different SO_2 concentrations and seed particles (a: no seed, b: NaCl, c: $(NH_4)_2SO_4$).

For the gas phase: The decays of guaiacol, NO_x, and SO_2 as a function of irradiation time are shown in Figure R8, Figure R9, and Figure R10, respectively, which have the similar changing trends for different experiments. The time-series variations in the concentrations of acetic acid at different SO_2 concentrations measured by the HR-ToF-PTRMS are shown in Figure R11, which shows that acetic acid concentration decreases with the increase of SO_2 concentration, suggesting that the uptake of acetic acid might be enhanced in the presence of sulfate and seed particles.

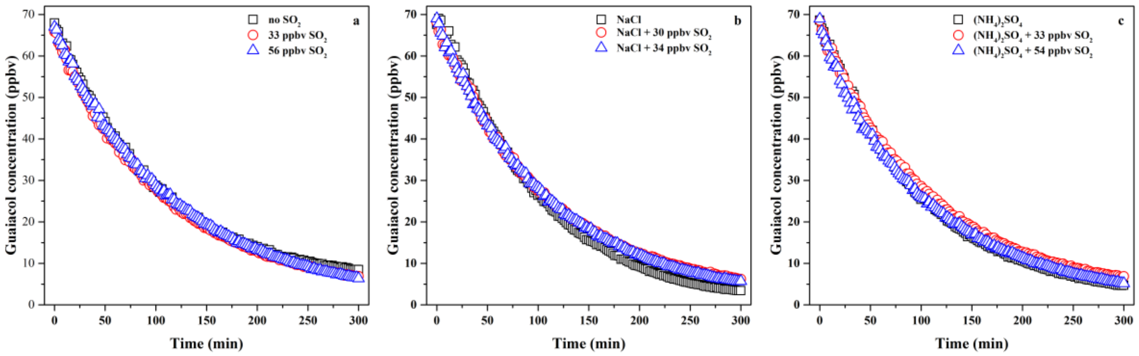

Figure R8. Decays of guaiacol as a function of irradiation time at different conditions (a: no seed, b: NaCl, c: $(NH_4)_2SO_4$)).

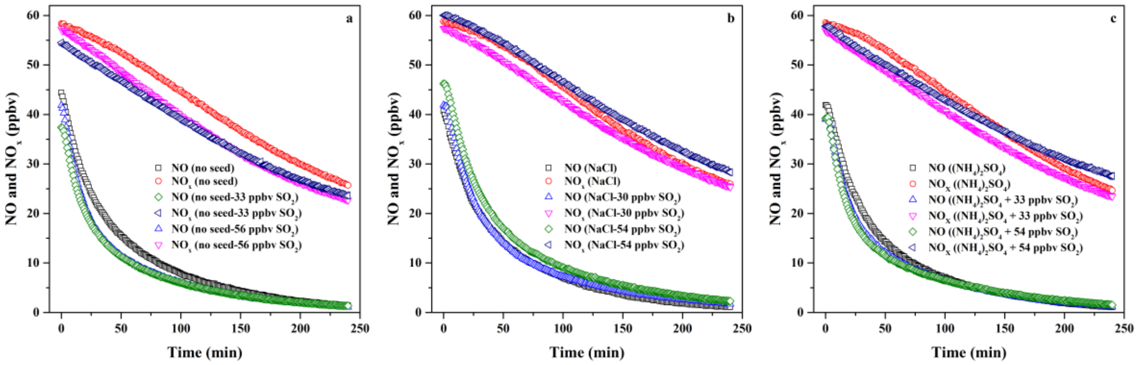

Figure R9. Decays of NO_x as a function of irradiation time at different conditions (a: no seed, b: NaCl, c: $(NH_4)_2SO_4$)).

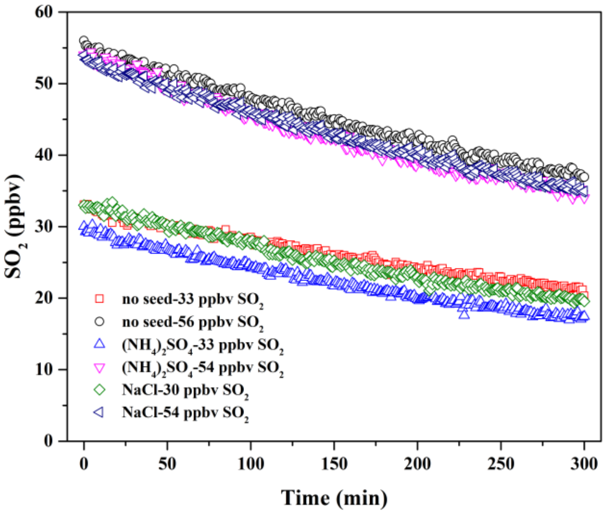

Figure R10. Decays of SO_2 as a function of irradiation time with different seed particles.

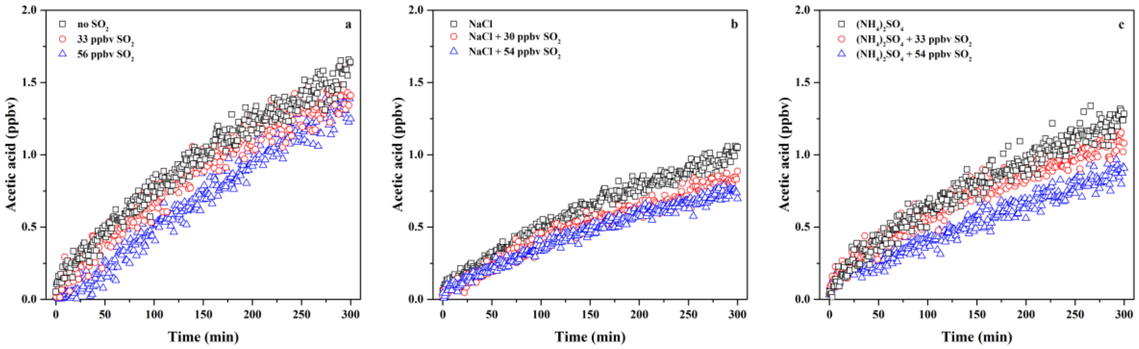

Figure R11. Variations in the gas-phase concentrations of acetic acid as function of irradiation time in the presence of various seed particles and SO_2 concentrations (a: no seed, b: NaCl, c: $(NH4)_2SO_4$).

Revisions in the manuscript:

1. Figures R1-R11 have been added in the revised Supplement.

2. Lines 245-251, Add: "the time-series variations in the concentrations of sulfate and nitrate are shown in Fig. S4. The decays of guaiacol, NO_x, and SO_2 are shown in Fig. S5a, Fig. S6a, and Fig. S7, respectively, which have the similar changing trends for different experiments. As illustrated in Fig. 2, the induction period became shorter with the increase of SO_2 concentration. The similar results caused by SO_2 have also been reported previously (Chu et al., 2016; Liu et al., 2016b)."

3. Lines 270-274 Add: "The time-series changes in the concentration of ammonium salt at different SO_2 concentrations are shown in Fig. S8. Its concentration increased obviously with increasing SO_2 concentration, suggesting that the more amounts of $(NH_4)_2SO_4$ was produced. The similar results have also been reported recently by Chu et al. (2016)."

4. Lines 295-296, Add: "The variations in H/C, O/C, and N/C ratios as a function of irradiation time are shown in Fig. S10."

5. Lines 308-311, Add: "This is well supported by the time-series variations in the fraction of organic ion groups (CH^+, CHO^+, and CHO^+_{gt1}) (Fig. S12a), which shows the higher fraction of CHO^+_{gt1} and lower fraction of CH^+ obtained at higher SO_2 concentration, consequently resulting in higher OS_C of SOA."

6. Lines 342-349, Add: "This is well supported by the time-series variations in the concentrations of acetic acid at different SO_2 concentrations measured by the HR-ToF-PTRMS (Fig. S15a), which shows that acetic acid concentration decreased with the increase of SO_2 concentration (0−56 ppbv). These results were in good agreement with those reported by Liggio et al. (2005) and Liu et al. (2010), who observed that that the uptake of organic compounds under acidic conditions would be enhanced significantly. Recently, Huang et al. (2016) have also reported that acetic acid is present in SOA formed via α-pinene ozonolysis and its uptake would increase in the presence of seed particles."

7. Line 361, Add: "(i.e., shorten induction period)"

8. Lines 385-390, Add: "As shown in Figs. S12b and S12c, compared to $(NH_4)_2SO_4$ seed particles, the higher fraction of CHO^+_{gt1} and lower fraction of CH^+ were obtained with NaCl seed particles, consequently resulting in higher OS_C of SOA. The time-series evolution of O/C, H/C, and N/C ratios is shown in Figs. S16 and S17, which indicate that O/C ratio with NaCl seed particles is higher than that with $(NH_4)_2SO_4$ seed particles."

9. Lines 405-409, Add: "As shown in Fig. S15, the concentration of acetic acid in the gas phase with NaCl seed particles was lower than that with $(NH_4)_2SO_4$ seed particles.

It suggests that the uptake of acetic acid on NaCl seed particles might be higher than that on $(NH_4)_2SO_4$ seed particles under the similar experimental conditions (i.e., NO_x and guaiacol concentrations, temperature, and RH)."

10. Lines 431-435, Add: "The decays of guaiacol, NO_x, and SO_2 are shown in Fig. S5, Fig. S6, and Fig. S7, respectively, which have the similar changing trends for different experiments. Fig. S19 shows the time-series evolution in the sulfate concentration in the presence of different SO_2 concentrations and seed particles, which indicates that sulfate concentration is dependent on SO_2 concentration."

11. Lines 437-438, Add: "but had an ignorable impact on the induction period"

12. Lines 451-455, Add: "which was well supported by the time-series variations in H/C, O/C, and N/C ratios at different SO_2 concentrations with NaCl and $(NH_4)_2SO_4$ as seed particles, shown in Figs. S16 and S17. In addition, as shown in Figs. S12b and S12c, the higher fraction of $\mathrm{CHO}^{+}_{\mathrm{gt1}}$ and lower fraction of CH^{+} were obtained at higher SO_2 concentration, consequently resulting in higher $\mathrm{OS_C}$ of SOA."

13. Line 467-471, Add: "This hypothesis could be supported by the variations in acetic acid concentration in the presence of different seed particles and SO_2 concentrations (Fig. S15), which shows that acetic acid concentration decreased with the increase of SO_2 concentration (0−54 ppbv)."

14. The revisions of the discussion about $\bar{\tau}_{\text{g-p}}$ and $\tau_{\text{g-w}}$ were showed as follows:

(1) Lines 25-27, Add: "According to the ratio of the average gas-particle partitioning timescale ($\bar{\tau}_{\text{g-p}}$) over the course of experiment to the vapor wall deposition timescale ($\tau_{\text{g-w}}$), the determined SOA yields were underestimated by a factor of ~2 times."

(2) Lines 32-34, Add: "The decreasing trend of $\overline{\tau}_{\text{g-p}} / \tau_{\text{g-w}}$ ratio in the presence of seed particles and SO_2 suggested that more SOA-forming vapors were partitioned onto particle phase, consequently increasing SOA yields."

(3) Lines 158-167, Add:

2.4 Vapor wall-loss correction

Previous studies have indicated that the losses of SOA-forming vapors to chamber wall can result in the substantial and systematic underestimation of SOA (Zhang et al., 2014, 2015). Therefore, SOA yields obtained in this work were also corrected by vapor wall loss. The effect of vapor wall deposition on SOA yields mainly depends on the competition between the uptake of organic vapors by aerosol particles and the chamber wall (Zhang et al., 2015). Thus, the ratio of the average gas-particle partitioning timescale ($\overline{\tau}_{\text{g-p}}$) over the course of experiment to the vapor wall deposition timescale ($\tau_{\text{g-w}}$) could be reasonably used to evaluate the underestimation of SOA yields. The detailed calculation of $\overline{\tau}_{\text{g-p}}$ and $\tau_{\text{g-w}}$ was shown in the Supplement.

(4) Lines 203-210, Add: "According to the ratios of $\overline{\tau}_{\text{g-p}} / \tau_{\text{g-w}}$ (0.61−0.93), the determined SOA yields were underestimated by a factor of ~2 times, suggesting that vapor wall loss in the chamber could significantly affect SOA formation. The similar results were reported previously by Zhang et al. (2014), who indicated that SOA yields for toluene photooxidation were substantially underestimated by factors as much as 4 times, caused by vapor wall loss. As shown in Fig. 1, the vapor wall-loss corrected SOA yields were in the range of (15.24 ± 0.85)% to (50.89 ± 2.87)%, and could also be reproduced by a one-product model (R^2 = 0.96).”

(5) Vapor wall-loss corrected SOA yields have been added in Figure 1 in the revised manuscript, shown as Figure R12.

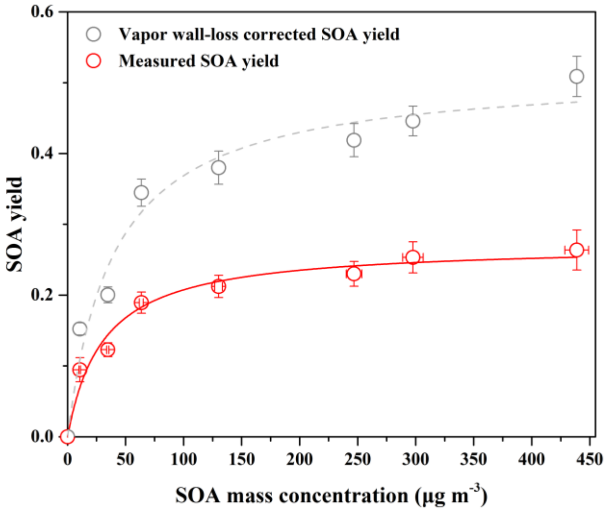

Figure R12. SOA yield as a function of SOA mass concentration (M_0) for guaiacol photooxidation in the presence of NO_x at different guaiacol concentrations. The solid lines was fit to the experimental data using a one-product model. Values of α and $K_{om,i}$ used to generate the solid line were (0.27 ± 0.01) and (0.033 ± 0.008) , and their values for the dot line were (0.52 ± 0.03) and (0.025 ± 0.006), respectively.

(6) The variations in $\overline{\tau}_{g\text{-}p} / \tau_{g\text{-}w}$ ratio in the presence of various seed particles as a function of SO_2 concentration has been added in the revised manuscript (Figure 3), as shown in Figure R13.

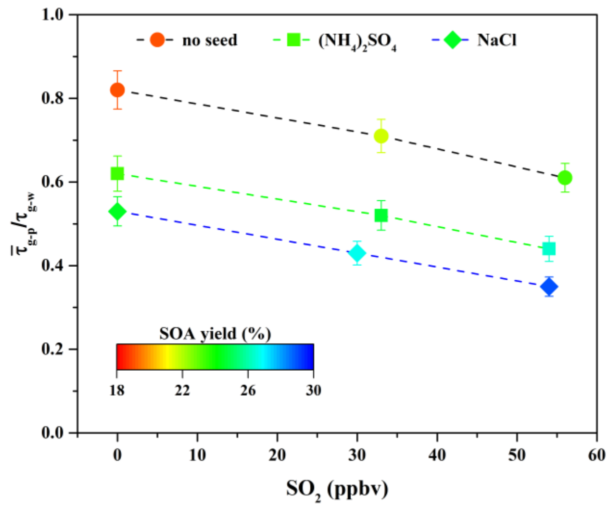

Figure R13. Variations in $\overline{\tau}_{\text{g-p}} / \tau_{\text{g-w}}$ ratio in the presence of various seed particles as a function of SO_2 concentration.

(7) Lines 248-251, Add: "As illustrated in Fig. 2, the induction period became shorter with the increase of SO_2 concentration. The similar results caused by SO_2 have also been reported previously (Chu et al., 2016; Liu et al., 2016b)."

(8) Lines 259-264, Add: "As shown in Fig. 3, $\overline{\tau}_{\text{g-p}} / \tau_{\text{g-w}}$ ratio decreased from 0.82 to 0.71 and 0.61 when SO_2 concentration increased from 0 to 33 and 56 ppbv. It suggests that the formed sulfate via SO_2 oxidation could serve as seed particles (Jaoui et al., 2008) and increase the surface areas of particles (Xu et al., 2016). These roles are favorable to partition more SOA-forming vapors onto particle phase (Zhang et al., 2014), consequently enhancing SOA yields."

(9) Lines 370-374, Add: "As shown in Fig. 3, $\overline{\tau}_{\text{g-p}} / \tau_{\text{g-w}}$ ratios with $(NH_4)_2SO_4$ and NaCl seed particles were 0.62 and 0.54, respectively, which suggested that more SOA-forming vapors were partitioned onto particle phase in the presence of NaCl seed particles (Zhang et al., 2014), consequently resulting in relatively higher SOA yield."

(10) Lines 445-448, Add: "As shown in Fig. 3, $\bar{\tau}_{\text{g-p}} / \tau_{\text{g-w}}$ ratio had a decreasing trend when increasing SO_2 concentration in the presence of seed particles, suggesting that the underestimation of SOA yields caused by vapor wall loss was weakened significantly because of the additional sulfate formed from SO_2 oxidation."

(11) Lines 488-489, Add: "These yields were underestimated by a factor of ~2 times according to $\bar{\tau}_{\text{g-p}} / \tau_{\text{g-w}}$ ratios."

(12) Lines 495-497, Add: "The decreasing trend of $\bar{\tau}_{\text{g-p}} / \tau_{\text{g-w}}$ ratio in the presence of seed particles and SO_2 suggested that more SOA-forming vapors were partitioned onto particle phase, consequently increasing SOA yields."

(13) The descriptions of timescale calculation in the Supplement are as follows:

3 Timescale calculation

The average gas-particle partitioning timescale ($\bar{\tau}_{\text{g-p}}$) over the course of experiment could be expressed as Eq. (S1) (Zhang et al., 2014; Seinfeld and Pandis, 2006), and the vapor wall deposition timescale ($\tau_{\text{g-w}}$) is calculated using Eq. (S2) (Zhang et al., 2015).

$$\bar{\tau}_{\text{g-p}} = \frac{1}{2\pi \bar{N}_{\text{p}} \bar{D}_{\text{p}} D_{\text{gas}} F_{\text{FS}}} \tag{S1}$$

$$\tau_{\text{g-w}} = \frac{1}{k_{\text{w}}} \tag{S2}$$

$$k_{\text{w}} = \left(\frac{A}{V}\right)\left(\frac{\alpha_{\text{w}} \bar{c} / 4}{\pi \alpha_{\text{w}} \bar{c} / 8 \left(D_{\text{gas}} k_{\text{e}}\right)^{0.5} + 1}\right) \tag{S3}$$

where $\bar{N}_{\text{p}}$ is the average particle number concentration for the whole experimental process since UV lamps were turned on, $\bar{D}_{\text{p}}$ is the number mean diameter, D_{gas} is the gas-phase diffusivity, F_{FS} is the Fuchs-Sutugin correction to the mass transfer flux due to noncontinuum effects and imperfect accommodation (Seinfeld and Pandis, 2006), k_{w} is the overall wall loss rate of organic vapor (Eq. (S3)), A/V is the surface to volume ratio of the chamber, α_{w} is the mass accommodation coefficient of eddy diffusion (~10^{-5}) (Zhang et al., 2014; Matsunaga and Ziemann, 2010), $\bar{c}$ is the mean thermal speed of the molecules, and k_{e} is the coefficient of eddy diffusion (0.015 $\mathrm{s^{-1}}$) (Zhang et al., 2014).

It is assumed that D_{gas} of organic vapor changes with the molecular weight (MW) and is equal to $D_{\mathrm{CO_2}}(\mathrm{MW_{CO_2}}/\mathrm{MW})$. The value of $D_{\mathrm{CO_2}}$ is 1.38×10^{-5} $\mathrm{m^2\ s^{-1}}$ (Zhang et al., 2014). Conventionally, MW of 98 g $\mathrm{mol^{-1}}$ (H_2SO_4) is widely used for the Fuchs-Sutugin correction, but a number more like 300 g $\mathrm{mol^{-1}}$ might be more representative of the condensable organic vapors. Thus, MW of 300 g $\mathrm{mol^{-1}}$ was selected in this work. The Fuchs-Sutugin correction is expressed as the following equation:

$$F_{\mathrm{FS}} = \frac{0.75\alpha(1+Kn)}{Kn^2 + Kn + 0.283Kn\alpha + 0.75\alpha} \qquad \text{(S4)}$$

where α is the mass accommodation coefficient onto particles (~0.002) (Zhang et al., 2014) and Kn is the Knudsen number, expressed as follows:

$$Kn = \frac{\lambda}{R_{\mathrm{p}}} \qquad \text{(S5)}$$

R_{p} is the particle radius and λ is the gas mean free path, which is calculated using Eq. (S6):

$$\lambda = \frac{3D_{\mathrm{gas}}}{\bar{c}} \qquad \text{(S6)}$$

$$\bar{c} = \sqrt{\frac{8N_\mathrm{A}kT}{\pi \mathrm{MW}}} \tag{S7}$$

where N_A, k, and T are Avagadro's number, Boltzman constant, and temperature, respectively.

Comment 2: Error bars on the comparison plots (Figs 2, 4, 5, and 7) would really help with interpretation. Were replicate experiments at some of the same initial conditions run? How much variation was observed?

Response to comment 2: Error bars in the Figures 2, 4, 5, and 7 in the original manuscript have been added, which are determined by HR-ToF-AMS analysis. In addition, the uncertainties of SOA yields, M_o, and OS_C have been added in the revised manuscript.

Revisions in the manuscript:

1. Line 24, Change "(9.46−26.37%)" **To** "ranged from (9.46 ± 1.71)% to (26.37 ± 2.83)%"

2. Lines 202-203, Change "9.46−26.37%" **To** "(9.46 ± 1.71)% to (26.37 ± 2.83)%"

3. Line 252, Change "63.62 to 71.88 and 78.59" **To** "(63.62 ± 1.71) to (71.88 ± 1.43) and (78.59 ± 2.06)"

4. Line 254, Change "The corresponding SOA yield increased by 14.05% and 23.66%, respectively." **To** "The corresponding SOA yields were (9.46 ± 1.71)%, (21.60 ± 1.27)%, and (23.42 ± 1.80)%, respectively."

5. Lines 365-366, Change "63.62 to 79.44 and 84.91" **To** "(63.62 ± 1.71) to (79.44 ± 1.86) and (84.91 ± 2.01)"

6. Lines 367-368, Change “The corresponding SOA yield increased by 23.06% and 29.57%, respectively.” **To** “The corresponding SOA yields were (23.31 ± 1.59)% and (24.54 ± 1.73)%, respectively.”

7. Lines 439-440, Change “M_0 was enhanced by 41.43% and 53.47%” **To** “M_o increased from (63.62 ± 1.71) to (90.89 ± 2.28) and (98.86 ± 2.11) μg m^{-3}.”

8. Lines 441-442, Change “the corresponding SOA yield increased by 41.43% and 53.47%” **To** “the corresponding SOA yields were (26.78 ± 1.97)% and (29.06 ± 1.82)%.”

9. Lines 442-445, Change “M_0 was enhanced by 32.58% for 33 ppb SO_2 and 41.34% for 54 ppb SO_2, respectively, and the corresponding SOA yield increased by 29.78% and 39.24%.” **To** “M_o increased from (63.62 ± 1.71) to (84.35 ± 2.09) for 33 ppbv SO_2 and (89.92 ± 2.31) μg m^{-3} for 54 ppbv SO_2, enhanced by 32.58% and 41.34%, respectively, and the corresponding SOA yields were (24.58 ± 1.78)% and (26.37 ± 1.98)%.”

10. Line 487, Change “9.46−26.37%” **To** “(9.46 ± 1.71)% to (26.37 ± 2.83)%”

11. Tables and Figures: The uncertainties of M_o, SOA yields, and OS_C have been added in Tables 1 and 2, as well as Figures 1, 2, 5, 6, and 8 in the revised manuscript.

Comment 3: What is the motivation for the PMF analysis? The difference between the two factors appears to be dominated by the intensity difference for CO_2^+. Do you expect a difference in chemical formation/aging when SO_2 is added? It looks like there is a difference in the chemical properties of the aerosol as a function of time for the different systems (Figure S4). Is this due to different chemistry or differences in partitioning of condensable vapors to the particles? Please also include more information on how the PMF analysis was carried out in the supplemental.

Response to comment 3: In order to further identify the effect of SO_2 on the chemical properties of SOA, positive matrix factorization (PMF) analysis for all AMS data obtained at different SO_2 concentrations over the course of experiments was carried out. The PMF analysis has been added in the Supplement. The detailed revisions were pointed out as follows.

In this work, we compared the effect of sulfate formed via SO_2 oxidation on SOA formation with/without seed particles. The results showed that the physical and chemical factors could be both helpful to enhance SOA yield, but their contributions were very difficult to quantify. It is well known that sulfate formed via SO_2 oxidation could serve as seed particles (Jaoui et al., 2008), increase the surface areas and change the composition of particles (Xu et al., 2016). All of these factors are favorable to partition more SOA-forming vapors onto particle phase (Zhang et al., 2014), consequently enhancing SOA yields. Therefore, the average gas-particle partitioning timescale ($\bar{\tau}_{\text{g-p}}$) over the course of experiment and the vapor wall-loss timescale ($\tau_{\text{g-w}}$) under different experimental conditions were estimated and discussed in the revised manuscript. Based on $\bar{\tau}_{\text{g-p}} / \tau_{\text{g-w}}$ ratio, the underestimation of SOA yield caused by vapor wall loss could be determined. The detailed revisions of the discussion about $\bar{\tau}_{\text{g-p}}$ and $\tau_{\text{g-w}}$ have been pointed out in the response to the Referee #3's Comment 1, thus these revisions were not listed.

Revisions in the manuscript:

Supplement, PMF analysis has been added as follows:

2 Positive matrix factorization (PMF) analysis

Positive Matrix Factorization (PMF) is a receptor model and a multivariate factor analysis tool, which could decompose a matrix of speciated sample data into two matrices, namely factor contributions and factor profiles (Paatero, 1997). In recent years, the PMF model was widely used for the analysis of high resolution (HR) mass spectra data, which could provide better separation of different organic components (DeCarlo et al., 2010; Docherty et al., 2008). This model is expressed as a bilinear factor model, namely, $x_{ij} = \sum_p g_{ip} f_{pj} + e_{ij}$, where i and j refer to values of j species in i samples, respectively, p is the number of factors in the solution and is used a least-squares fitting process to minimize the quality of fit parameter. In this work, the HR mass spectra (m/z 12–115) was analyzed by the PMF software coupled with a modified version of the CU AMS PMF Execute Calcs Tool version 2.06 developed by Ulbrich et al. (2009). The concentration and uncertainty matrices input into the PMF analysis were generated from the PIKA version 1.15D. Ions were classified and down-weighted according to the signal to noise ratios (SNR). $0.2 < SNR < 2$ was classified as the weak ions and down-weighted by a factor of 2, $SNR < 0.2$ was bad ions and removed from the analysis, and the uncertainty values of CO_2^+-related peaks at m/z 16 (O), 17 (HO), 18 (H_2O), 28 (CO), and 44 (CO_2) were down-weighted.

Comment 4: You claim that oligomerization reactions will decrease the oxidation state of the SOA (page 12, line 236). How does this occur (please either explain or provide references)? Oligomerization should lead to an increase in carbon number but little change in the net O/C or H/C values for the oligomer.

Response to comment 4: According to your valuable suggestion, this sentence has been rewritten in the revised manuscript.

Revision in the manuscript:

Line 316, Change “the oxidation state of SOA will decrease” **To** “the carbon number of oligomers will increase but their net O/C or H/C values have little change, consequently resulting in little change in the oxidation state of SOA (Chen et al., 2011).”

Comment 5: How are the spectra in Figures S5, S9, and S10 normalized? Are they normalized to the max intensity or to the sum of the intensities? It looks like there is very little negative ion intensity in many of the figures which I would not expect if these are normalized to the sum. When are these mass spectra taken from in terms of experiment time? Are they the average over the whole or the end only? Please also increase the size of this figure, it is very difficult to read which m/z values are negative.

Response to comment 5: All the spectra shown in Figures are the average spectra over the course of the experiment, which are normalized to the sum of the intensities. The little negative ions in the figures might be caused by the functionalization and oligomerization reactions, which were both enhanced in the presence of SO_2. But, we observed that increasing SO_2 concentration was in favor of improving the carbon oxidation state (OS_C) of SOA, indicating that the functionalization reaction should be more dominant than oligomerization reaction in this work. In addition, the size of these figures has been increased in the Supplement.

Comment 6: Please briefly outline how organosulfate concentration was calculated (page 13, line 251). In figure S6, what is the system being shown? Is this methyl sulfate alone or is it a mixture? If it is methyl sulfate alone, why are there so many oxidized and reduced nitrogen peaks fit under the curve? When fitting AMS data, it is best to use the smallest number of ions to fit the curve as you can always improve the fit by adding more ions.

Response to comment 6: Figure S6 in the original Supplement is taken from smog chamber experiment. In order to describe accurately, its caption has been revised in the revised Supplement and the experiment which the figure is taken from has been added in the suitable position in the revised manuscript. In addition, the calculation of organosulfate concentration has been added in the Supplement. The detailed revisions were pointed out as follows.

We agree that it is best to use the smallest number of ions to fit the curve. However, we found that if the N-containing peaks were not included during the fitting AMS data process, the fit result was not satisfactory. Thus, the N-containing peaks were taken into account during the fitting process. In addition, the significant N/C ratios were observed in this work, suggesting that organic N-containing compounds were produced via guaiacol photooxidation in the presence of NO_x.

Revisions in the manuscript:

1. Line 339, Add: “(Exp. 3 in Table 2)”

2. Caption of Figure S14, Change “Fitted peaks of average W-mode mass spectrum of methyl sulfate obtained at 56 ppb SO_2 without seed particles.” **To** “Fitted peaks of average W-mode mass spectrum of methyl sulfate obtained from smog chamber experiment with 56 ppbv SO_2 and no seed particles.”

3. Supplement. The calculation of organosulfate concentration has been added as follows:

4 Organosulfate concentration calculation

Considering that methyl sulfate is the simplest organosulfate, the fraction of $C_xH_yO_zS$ is more likely to be lower than that of methyl sulfate (Huang et al., 2015). In addition, more information about the varieties of organosulfates could not be obtained in this work. Therefore, a conservative low-bound of organosulfate concentration has been estimated according to the method described by Huang et al. (2015), as shown in Eq. (S8).

$$C_{\mathrm{OS_{min}}} = f_{\mathrm{OS}} \times (C_{\mathrm{org}} + C_{\mathrm{SO_4}}) \qquad \text{(S8)}$$

$$f_{\mathrm{OS}} = \frac{\dfrac{\sum_h I_{\mathrm{OS},h}}{\mathrm{RIE_{OS}}}}{\dfrac{\sum_n I_{\mathrm{org},n}}{\mathrm{RIE_{org}}} + \dfrac{\sum_t I_{\mathrm{SO_4},t}}{\mathrm{RIE_{SO_4}}}} \qquad \text{(S9)}$$

where $C_{\mathrm{OS_{min}}}$ is the minimum concentration of organosulfates; f_{OS} is the factor that represents for the fractional contribution of organosulfates to the lumped species of organics and sulfate in W-mode data; C_{org} and $C_{\mathrm{SO_4}}$ are the concentrations of organics and sulfate calculated from V-mode data, respectively; *h, n, and t* indicate the fragments of organosulfates, organics, and sulfate, respectively; $\sum_h I_{\mathrm{OS},h}$, $\sum_n I_{\mathrm{org},n}$, and $\sum_t I_{\mathrm{SO_4},t}$ are the total signal intensities of organosulfates, organics, and sulfate, respectively, obtained from W-mode data; $\mathrm{RIE_{OS}}$ is the relative ionization efficiency for organosulfates, which is estimated as the average of $\mathrm{RIE_{org}}$ = 1.4 and $\mathrm{RIE_{SO_4}}$ = 1.2 (Barnes et al., 2006).

Comment 7: You note on line 267, page 13 that you do not see evidence of H_2SO_4 formation. Is this conclusion drawn from a lack of the ion(s) observed in the AMS? Have you run acidified ammonium sulfate particles? How do the mass spectra of the sulfate peaks from acidified ammonium sulfate measured in your AMS compare to the sulfate peaks observed here?

In Table 2 you note that the sulfate concentration formed via SO_2 oxidation increases with more SO_2 in the chamber (~10-20 ug/m^3). You also note that the organosulfate concentration was in the range of 2.1-4.3 ng/m^3 (page 13, line 250). What is the identity of the remaining sulfate in the particles (ammonium sulfate, sulfuric acid)? Going back to the first question, what does its time trace look like?

Response to comment 7: In the original manuscript, we wanted to express that new particle formation by H_2SO_4 was not observed using a SMPS. However, we observed the significant formation of sulfate by AMS, and the time-series changes in the sulfate concentration with different seed particles are shown in Figure R14. Since it is difficult to completely remove trace NH_3 in the zero air, thus the formed sulfate should be the mixture of H_2SO_4 and $(NH_4)_2SO_4$. The time-series changes in the concentration of ammonium salt at different SO_2 concentrations are shown in Figure R2. Its concentration increases obviously with increasing SO_2 concentration, suggesting that the more amounts of $(NH_4)_2SO_4$ are produced. In our study, SOA is rapidly formed via guaiacol photooxidation when UV lamps are turned on, thus the new particle formation attributed to sulfuric acid formed via SO_2 oxidation was not observed by the SMPS during experimental process. In order to describe accurately, some revisions have been made in the revised manuscript.

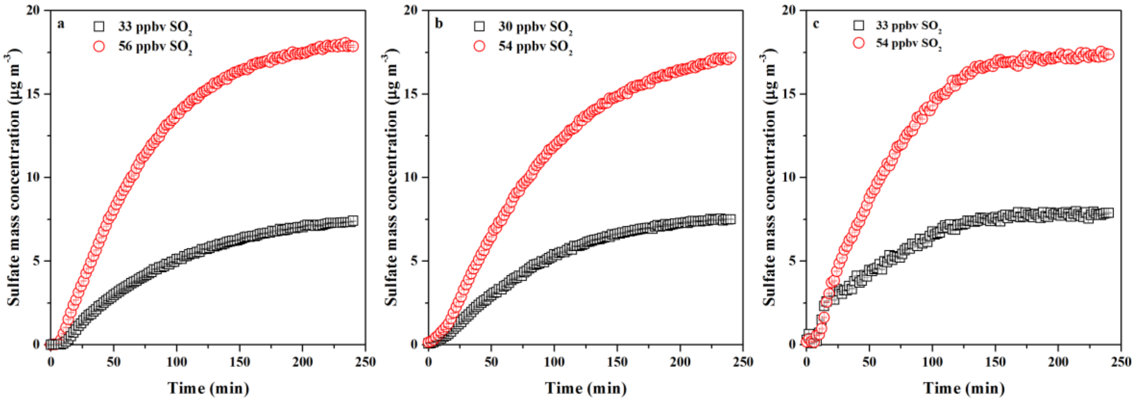

Figure R14. Variations in the concentrations of sulfate as function of irradiation time in the presence of various seed particles and SO_2 concentrations (a: no seed, b: NaCl, c: $(NH_4)_2SO_4$). The sulfate concentrations shown in Figure R1c is the net concentrations formed via SO_2 oxidation, e.g., do not include the $(NH_4)_2SO_4$ concentration added in the smog chamber.

Revisions in the manuscript:

1. Figure R14 has been added in the Supplement.

2. Lines 266-274, Add: "Nevertheless, the particle peak attributed to sulfate formed via SO_2 oxidation was not observed by the SMPS during experimental process due to the quick particle growth in the presence of organic vapors. In this work, it is difficult to completely remove trace NH_3 from zero air, thus the formed sulfate should be the mixture of H_2SO_4 and $(NH_4)_2SO_4$. The time-series changes in the concentration of ammonium salt at different SO_2 concentrations are shown in Fig. S8. Its concentration increased obviously with increasing SO_2 concentration, suggesting that the more amounts of $(NH_4)_2SO_4$ was produced. The similar results have also been reported recently by Chu et al. (2016)."

Comment 8: Even if the surface area of the aerosol particles is much smaller than that of the smog chamber (page 14 line 276) I would still expect that small increases in the surface area of particles for condensation would have an effect on SOA yield. Your data for surface area and SOA yield appears to follow a relatively linear trend. Can you run an experiment with the same initial surface area with and without SO_2? (i.e. start with higher initial seed in the experiment without SO_2). This will help interpret the influence of SO_2 on SOA yield.

Response to comment 8: Thank you very much for your constructive suggestion, the increase in the surface area of particles for SOA-forming vapor condensation is discussed in the revised manuscript according to the ratios of $\overline{\tau}_{\text{g-p}} / \tau_{\text{g-w}}$. The results show that $\overline{\tau}_{\text{g-p}} / \tau_{\text{g-w}}$ ratio decreases from 0.82 to 0.71 and 0.61 when SO_2 concentration increases from 0 to 33 and 56 ppbv. These suggest that more SOA-forming vapors are in favor of partitioning onto particle phase (Zhang et al., 2014), consequently enhancing SOA yields.

Revisions in the manuscript:

1. Lines 259-264, Add: "As shown in Fig. 3, $\overline{\tau}_{\text{g-p}}/\tau_{\text{g-w}}$ ratio decreased from 0.82 to 0.71 and 0.61 when SO_2 concentration increased from 0 to 33 and 56 ppbv. It suggests that the formed sulfate via SO_2 oxidation could serve as seed particles (Jaoui et al., 2008) and increase the surface areas of particles (Xu et al., 2016). These roles are favorable to partition more SOA-forming vapors onto particle phase (Zhang et al., 2014), consequently enhancing SOA yields."

2. Lines 445-448, Add: "As shown in Fig. 3, $\overline{\tau}_{\text{g-p}}/\tau_{\text{g-w}}$ ratio had a decreasing trend when increasing SO_2 concentration in the presence of seed particles, suggesting that the underestimation of SOA yields caused by vapor wall loss was weakened significantly because of the additional sulfate formed from SO_2 oxidation."

Comment 9: In Figure 6, the intensity of CO^+ does not match the intensity of CO_2^+. What frag tables are being used to calculate the CO^+ ion? Usually, that is set at the same value as CO_2^+ because of interference from atmospheric N_2^+. When (during the experiment) are these mass spectra collected? Are they an average over the whole or the end of the experiments? How reproducible are these differences? Is the difference spectra shown in Figure 6c observed for all the combinations of NaCl and ammonium sulfate seeds (at the same SO_2 concentrations)?

Response to comment 9: Figure 6 in the original manuscript shows the average mass spectra over the course of experiments. The difference spectrum shown in Figure 6c is obtained without SO_2. We are very sorry to make a mistake about the wrong expression in Figure 6 and Figure S8 in the original versions. We double checked the MS data. The intensities of m/z 44 shown in Figure 6 and Figure S8 were obtained by selecting the “Sum to UMR” during the output process of mass spectra, which were the total intensities of all fragments at m/z from 43.981 to 44.026. Thus, the intensities of CO^+ and CO_2^+ do not match in our original figures. The corrected figures have been added in the revised manuscript and Supplement, as shown in Figures R15 and R16. The detailed revisions were listed as follows.

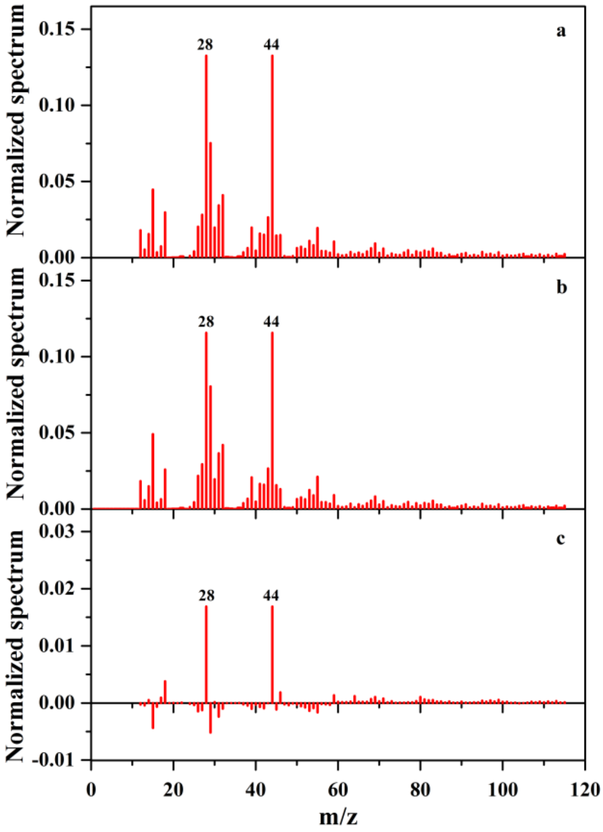

Figure R15. Mass spectra of SOA with NaCl (a) and $(NH_4)_2SO_4$ (b) as seed particles obtained by HR-ToF-AMS, as well as their difference mass spectrum (c) obtained by a minus b.

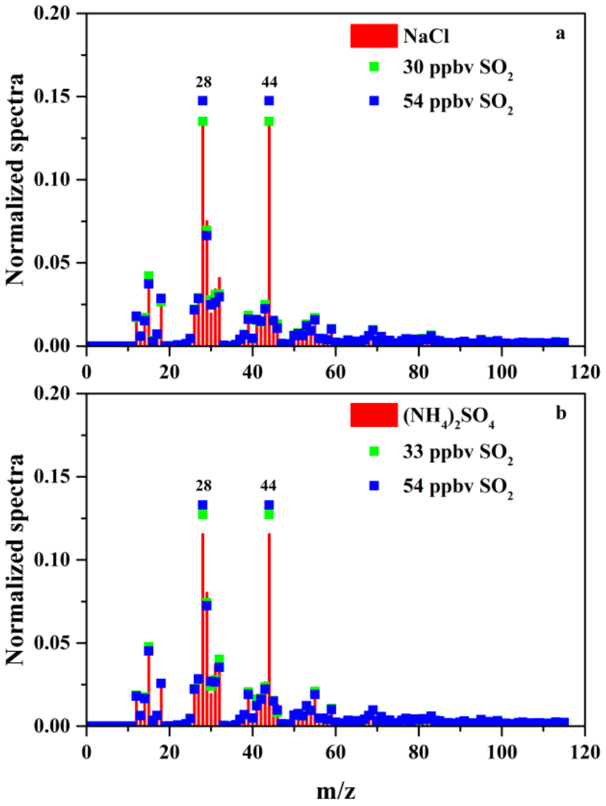

Figure R16. Mass spectra of SOA with NaCl (a) and $(NH_4)_2SO_4$ (b) as seed particles obtained by HR-ToF-AMS at different SO_2 concentration (red bars: without SO_2; olive markers: 30 ppbv SO_2 for a and 33 ppbv SO_2 for b; blue markers: 54 ppbv SO_2).

Revisions in the manuscript:

Figure S15 has been added in the revised manuscript (Figure 7).

Figure R16 has been added in the revised Supplement (Figure S20).

References

Jaoui, M., Edney, E. O., Kleindienst, T. E., Lewandowski, M., Offenberg, J. H., Surratt, J. D., and Seinfeld, J. H.: Formation of secondary organic aerosol from irradiated alpha-pinene/toluene/NO_x mixtures and the effect of isoprene and sulfur dioxide, J. Geophys. Res.-Atmos., 113, doi: 10.1029/2007jd009426, 2008.

Xu, L., Middlebrook, A. M., Liao, J., de Gouw, J. A., Guo, H., Weber, R. J., Nenes, A., Lopez-Hilfiker, F. D., Lee, B. H., Thornton, J. A., Brock, C. A., Neuman, J. A., Nowak, J. B., Pollack, I. B., Welti, A., Graus, M., Warneke, C., and Ng, N. L.: Enhanced formation of isoprene-derived organic aerosol in sulfur-rich power plant plumes during Southeast Nexus, J. Geophys. Res.-Atmos., 121, 11137-11153, doi: 10.1002/2016jd025156, 2016.

Zhang, X., Cappa, C. D., Jathar, S. H., McVay, R. C., Ensberg, J. J., Kleeman, M. J., and Seinfeld, J. H.: Influence of vapor wall loss in laboratory chambers on yields of secondary organic aerosol, Proc. Natl. Acad. Sci. U. S. A., 111, 5802-5807, doi: 10.1073/pnas.1404727111, 2014.